ORIGINAL RESEARCH

Kombucha Tea By-product as Source of Novel Materials: Formulation and Characterization of Films

Yuly A. Ramírez Tapias[1,2] · Mercedes A. Peltzer[1,2] · Juan F. Delgado[1,2] · Andrés G. Salvay[1]

Abstract

The development of biodegradable materials from microbial exopolysaccharides has extraordinary potential to be applied in food packaging. Kombucha tea is a fermented drink produced by a symbiotic community of bacteria and yeasts, where a by-product based on bacterial cellulose is generated at the surface of the beverage. In this work, novel materials based on the integral kombucha tea by-product were developed from the floating and the intentionally submerged discs of biomass. Each disc was dispersed in water and subjected to ultrasonic homogenization. Films obtained by casting exhibited high homogeneity without cracks with a microstructure composed by a homogeneous and continuous cellulosic matrix of ribbon-shaped nanofibers. Infrared spectroscopy and thermogravimetric analyses indicated the further presence of low and high molecular weight compounds. The increase in glycerol content in the film decreased glass transition temperature and increased flexibility, hydration, and water vapor permeability. Films obtained from submerged discs had an additional plasticization given by substances incorporated during the immersion in the culture medium. Both types of films made from the floating and the submerged disc had a natural and remarkable antioxidant activity of $69 \pm 2\%$ and $72 \pm 2\%$ of radical inhibition, respectively, probably due to polyphenols or other compounds from the culture medium. Results revealed that using the integral cellulosic by-product of kombucha tea to prepare films could be advantageous due to the cost-effective process (no separation, no purification), interesting physical–chemical properties, and the retention of natural bioactive substances.

Keywords Biobased films · Kombucha · Bacterial cellulose · Antioxidant activity · Plasticization · Glass transition

Introduction

The use of biobased packaging materials has emerged as an innovative alternative to materials produced from non-renewable and non-biodegradable resources (Johansson et al. 2012; Peltzer et al. 2017). The sources of biobased materials are those from biomass such as agricultural derivatives and biopolymers obtained from microorganisms' metabolism (Coma et al. 2019). In this regard, the study of new materials is principally focused on proteins and polysaccharides and on the physicochemical or biotechnological processes to convert these components to materials such as value-added films (Siracusa et al. 2008).

Depending on the type of biopolymers that compose the film, their mechanical, physicochemical, and thermal properties will differ, and they can provide diverse advantageous features for specific applications, especially for food packaging preservation (Peltzer et al. 2018a). Some general characteristics of these films are the thermal and mechanical performances and the feasibility to be a carrier of functional compounds, besides serving as a barrier with selective permeability to the transfer of substances such as oxygen, carbon dioxide, lipids, flavor components, and water vapor (Siracusa et al. 2008). These characteristics configure various synergic mechanisms to preserve foodstuff, improve appearance and handling, prevent loss of moisture or oxidation, and keep organoleptic properties (Peltzer et al. 2017).

✉ Mercedes A. Peltzer
mercedes.peltzer@unq.edu.ar

✉ Andrés G. Salvay
asalvay@unq.edu.ar

1   Departamento de Ciencia y Tecnología, Universidad Nacional de Quilmes, Roque Sáenz Peña 352, B1876BXD Bernal, Buenos Aires, Argentina

2   Consejo Nacional de Investigaciones Científicas y Técnicas (CONICET), Godoy Cruz 2290, C1425FQB Ciudad Autónoma de Buenos Aires (CABA), Argentina

In recent years, new materials based on biomass sources such as integral yeast cells (Delgado et al. 2016) and water kefir grains biomass (Coma et al. 2019) were developed. Polysaccharides as cellulose, chitosan, starch, dextran, pectin, alginate, carrageenan, pullulan, and kefiran are suitable biopolymers due to its film-forming ability (Cazón et al. 2017; Coma et al. 2019). The most abundant polysaccharide is cellulose obtained mainly from plants, which once extracted, it must be purified (Barud et al. 2011). The purification process to isolate pure cellulose from vegetable sources by removing impurities as lignin and hemicellulose, and the subsequent derivatization procedures to obtain modified cellulose as carboxymethyl cellulose or methylcellulose, is necessary to modulate mechanical and barrier properties (Cazón et al. 2017). But these processes are extremely energy demanding that normally induces polymer degradation, and also, the environmental impact of the by-products and residues of the process needs to be considered (Cerrutti et al. 2016).

Moreover, cellulose obtained from bacteria, especially those from the acetic acid group (AAB), synthesizes extracellular cellulose in the form of pure nanofibrils using glucose and ethanol as carbon source (Dourado et al. 2016). Among the different genera of this family, the *Acetobacter*, *Gluconacetobacter*, and *Komagataeibacter* genera are the most notable cellulose producers (Dourado et al. 2016). Cellulose from plants and bacterial cellulose have identical chemical structure, but because of the characteristics of fibers and its purity, bacterial cellulose has several advantages such as higher mechanical strength, crystallinity, and hydrophilicity (Rozenberga et al. 2016; Dima et al. 2017).

It has been reported that symbiotic relations between AAB and the acid-tolerant and osmophilic yeasts enhance cellulose yield production due to synergic microbial metabolism, while yeasts hydrolyze sucrose and consume glucose and fructose to produce ethanol, AAB oxidize it to acetic acid and also it is activated cellulose-synthase machinery, producing a pellicle in liquid–air interface under static conditions (Dourado et al. 2016; Gullo et al. 2018). Taking advantage from these symbiotic relations among microorganisms, kombucha tea fermentation emerges as an excellent opportunity to obtain bacterial cellulose because it is a natural symbiotic culture of bacteria and yeasts, usually known as SCOBY (symbiotic community of bacteria and yeasts) (Jayabalan et al. 2014).

The kombucha tea is a beverage that is obtained from the infusion of tea leaves by the fermentation of the SCOBY community; these microorganisms produce a thick cellulosic biofilm and a sparkling acidic broth used as a probiotic beverage that is commercialized. The kombucha tea and the biofilm have been increased in its popularity due to the therapeutic and prophylactic effects in human health, acting as a laxative, agent for the prevention of microbial infections, blood cleansing, and it facilitates to excretion of toxins (Jayabalan et al. 2014;

Dima et al. 2017). Food and Drug Administration (FDA, USA) have categorized the commercial production of kombucha tea in the Food Code as a specialized process. It means that it is necessary to have an approved food safety plan to start the production and ensure the non-toxicity for human consumption. Homemade preparation was the only scale of production by many years, but it is clear that in recent years, commercial kombucha tea became a relevant commercial activity. Dutta and Paul (2019) have made a non-exhaustive list of manufacturers, all of them established after 2008. Kim and Adhikari (2020) have published a list of 201 kombucha products in the USA, commercialized by different companies. Global kombucha market size has been estimated at US$1.67 thousand million in 2019 (Grand View Research 2020).

Therefore, there is a great opportunity to add value to the side stream of the process production of kombucha tea and convert this by-product in a new material source by using the integral biomass produced during fermentation. Using this cellulosic biofilm without additional downstream steps to obtain biobased materials, integral biomass is preserved and natural molecules from the culture medium can provide to the material other functional properties like antioxidant and antimicrobial activity (Dima et al. 2017; Cottet et al. 2020). It is to be expected that the integral by-product of kombucha tea fermentation composed mainly by bacterial cellulose can be processed in order to obtain films (Cottet et al. 2020).

Active food packaging with antioxidant activity is an effective way to prevent the spoilage arising from oxidation during storage (Muriel-Galet et al. 2014; Li and Ye 2017). The traditional approach to developing a film with antioxidant activity is to incorporate an antioxidant agent into the material (de Moraes Crizel et al. 2018; Li et al. 2018). However, negative effects on the mechanical properties of films (Sangatash et al. 2016), poor miscibility and phase separation during the film-forming process (Aziz and Almasi 2018), and the thermal or chemical degradation of the bioactive compounds during film production and food storage are the most common deficiencies of the direct addition of bioactive compounds into biodegradable active films (Aziz and Almasi 2018).

The aim of this study was to develop new biobased active materials from a natural antioxidant system, using the integral cellulosic by-product generated during the fermentation of kombucha tea. The effect of the position of the cellulosic disc (surface or immersed in the liquid) and the addition of glycerol in the formulations were evaluated on the microstructural, thermal, mechanical, hydration, water vapor barrier, and antioxidant properties of the films. This new approach for material development contributes to a more efficient process with less waste and allows exploiting the properties of whole biomass.

Materials and Methods

Chemical Materials

Analytical grade chemicals including ABTS (2,29-azinobis-(3-ethylbenzothiazoline-6-sulfonic acid)), potassium persulfate, and ethanol were obtained from Sigma-Aldrich (St. Louis, MO, USA). All salts used to preparation of saturated solutions were acquired in analytical grade from Merck (Darmstadt, Germany). Analytical grade glycerol and silica gel were purchased from Biopack (Buenos Aires, Argentina). Food grade sucrose (Ledesma, Buenos Aires, Argentina) was purchased in a local market.

Kombucha Tea Fermentation and By-product Recovery for Film Development

The native culture of kombucha tea LOMCEM MKO1 was obtained from a household at Villa Ballester (Argentina) and was used as the starter culture. The stock culture was maintained at static conditions at room temperature and subcultured periodically (30 ± 7 days) in a liquid medium based on black tea. The tea infusion was prepared from 7 g of organic black tea bags (Hierbas del Oasis, Argentina) into 1.5 L water at 80 °C during 10 min. After cooling to 22 °C, 150 g sucrose was dissolved and then the tea infusion was inoculated with 250 ml of stock culture. In order to maximize biomass production, a single batch with six simultaneous fermentations was carried out on independent glass vessels of 14 cm diameter covered with a cellulose cloth under static conditions at 22 °C. The initial pH of the culture was 4.28 ± 0.02 which excludes the growth of environmental microorganisms. After 21 days, the floating disc generated by kombucha tea fermentation was harvested and submerged in a new fermentation broth, in which a new floating disc was produced after 21 days. Both types of discs were recovered: the superficial disc was denominated K1 and the submerged one K2. The use of the floating and the intentionally submerged cellulose discs was proposed to compare the different properties of the obtained films, since substances present in the culture broth could be incorporated into the submerged material. Afterwards, both types of discs were washed with distilled water and sterilized at 121 °C and 101 kPa during 15 min in a steam autoclave. The amount of dry matter of the washed and sterilized discs was as 0.09 g per g for K1 and 0.10 g per g for K2. This was determined by drying at 105 °C during 3 h.

For film preparation, the discs were grinded by using a blender and finally filtered in vacuum using a Buchner funnel with filtration paper. In this way, the excess of water was removed. The amount of dry matter of the grinded and filtered materials was as 0.10 g per g for K1 and 0.12 g per g for K2.

Preparation of Films

Grinded and filtered kombucha disc K1 and K2 were used for the preparation of film-forming dispersions of 1.5 wt% dry matter of K1 and 1.5 wt% dry matter of K2 in distilled water. Both dispersions were firstly homogenized at 15,000 rpm during 5 min by using an Ultra-turrax T-25 (IKA, Germany). Then, they were subjected to ultrasonic homogenization (VCX-750, Sonics and Materials, Inc., USA) at 80 W during 15 min. These two homogenization processes were carried out a second time in order to produce a fine dispersion. Ultra-turrax homogenization improves material dispersion, while ultrasonic homogenization is necessary to disassemble the compact structure of the K1 and K2 fibers and cell wall of remaining microorganisms (Coma et al. 2019). With the purpose of study the effect of plasticizer on films properties, pure glycerol was added to dispersions K1 and K2 at levels of 0, 10, 20, and 30 wt% respect to dry matter (d.m.). After the addition of plasticizer, the dispersion was stirred during 15 min at room temperature. The final pH of the dispersions was 4.5.

In order to obtain films of thicknesses close to 0.1 mm, 40 g of dispersion was placed in each plastic Petri dish of 86 mm of diameter. Evaporation of water was done at 37 °C and 40% relative humidity (r.h.) by casting in a ventilated oven (Sanyo MOV 212F, Japan) until the remaining water content of the films was between 10 and 15%. Then, K1 and K2 films were stored at 22 °C and 43% r.h. Finally, according to the requirements of the experiment, the films were equilibrated at 22 °C in desiccators at different r.h. using saturated solutions of LiCl, $MgCl_2$, K_2CO_3, $Mg(NO_3)_2$, NaBr, NaCl, and $BaCl_2$, to generate conditions of 11, 33, 43, 52, 57, 75, and 90% r.h., respectively. Dried atmospheres were obtained using silica gel.

Visual Appearance, Quality Evaluation, and Thickness Measurements of the Films

The visual appearance of films was tested using a Samsung SM-J415G camera by taken photographs of the surface of samples at 20 cm in the zenithal plane and natural lighting. The quality of the films obtained was assessed considering aspects of handleability, homogeneity, and continuity in three independent replicates (Moraes et al. 2013). Film thickness was measured with a digital caliper ($\pm 10^{-6}$ m; 3109-25-E, Insize Co., China). Thickness was obtained using the average of 10 measurements for each specimen.

Microstructural Characterization

The microstructure of films was analyzed by using a scanning electron microscope Carl Zeiss NTS–SUPRA. Cross sections were obtained cutting the films at -80 °C with a sharp blade. Then all samples were placed in the specimen holder and

stored at 22 °C and 43% r.h. For best viewing under a microscope, the samples were coated with a gold layer. Images of the surfaces (3 kV and magnification × 25,000) and the cross sections (15 kV and magnification × 800) of unplasticized K1 and K2 films were acquired in high vacuum.

Fourier Transformed Infrared Spectroscopy Analysis

Infrared spectra of unplasticized K1 and K2 films were determined using a Fourier-Transformed Infrared Analyzer (FTIR) (Affinity-1, Shimadzu Co., Japan) equipped with an attenuated total reflectance diamond module (GladiATR, Pike Technologies, USA). Spectra were obtained in the range of 4000–400 cm^{-1} as an average of 60 scans with 4.0 cm^{-1} resolution and Happ-Genzel apodization. A blank spectrum was obtained before each test to compensate the humidity effect and the presence of carbon dioxide in the air. Spectra were obtained in duplicate.

Thermogravimetric Analyses

Mass loss in samples as a function of temperature was registered in a TA Instruments Q-500 (Delaware, USA) thermobalance. Approximately 10 mg of each sample was weighed in a platinum pan and heated. Unplasticized samples K1 and K2 were previously equilibrated at 90% r.h. and then located at the platinum pan and heated from 20 to 110 °C, at 1 °C min^{-1}, in order to study in detailed manner the loss of hydration water. To study the thermal degradation, samples K1 and K2 with different percentages of glycerol were heated at 20 °C min^{-1}, from 100 to 800 °C. Experiments were carried out in duplicate under nitrogen atmosphere (flow rate 60 ml min^{-1}). The temperature at the maximum degradation rate (T_{max}) was determined from the peak of derivative curves.

Differential Scanning Calorimetry

DSC thermograms of the films were measured using a Differential Scanning Calorimeter (TA Instruments Q200, Delaware, USA), in the range of − 80 to 150 °C, with a previous equilibration step at − 80 °C during 5 min, and then, temperature was increased at 10 °C min^{-1}. Approximately 7 mg of samples was placed into Tzero® aluminum pans and sealed with hermetic lids. Firstly, the effect of glycerol content was studied in samples K1 and K2 previously dehydrated in silica gel during 7 days. Secondly, the effect of hydration water was studied on unplasticized films hydrating the samples until reach the equilibrium in environments of 0, 52, 75, and 90% r.h. All the conditioning steps were performed at 22 °C. Glass transition temperatures (T_g) were determined using TA Universal Analysis software (v4.5, TA Instruments, USA), at the mid-point. Experiments were performed in triplicate ($n = 3$).

Mechanical Properties

Uniaxial tensile tests of films were performed in a Universal Testing Machine (TC-500 II-Series, Micrometric, Argentina) equipped with a 300-N cell. Sample probes were cut in rectangular shapes of 50 mm of length and 10 mm of width; the effective distance between jaws was 25 mm. Test were performed at 22 °C and specimens of K1 and K2 films with different percentages of plasticizer were previously conditioned at 52% of r.h. The selected speed to perform tests was 5 mm min^{-1}, and ten specimens of each composition were tested. Deformation at break e (%), maximum tensile strength TS_{max} (MPa), and elastic Young's modulus Y (MPa) were calculated from the resulting stress–strain curves as average of ten measurements ($n = 10$) according to ASTM D882 (1997).

Water Sorption Isotherms

Water sorption isotherms were determined gravimetrically at 22 °C according to standard procedure previously described (Delgado et al. 2018a). Dried samples of K1 and K2 films with a superficial area of 58 cm^2 and different percentages of glycerol were placed in desiccators of 1.5 L and equilibrated at different a_w. Samples were periodically weighed using an analytical balance ($\pm 10^{-4}$ g), and the evolution to the equilibrium at each moisture condition was monitored until constant weight. The water content or hydration h, given in units of grams of water per gram of dry matter (d.m.), was evaluated as a function of water activity a_w ($a_w = \%$ r.h./100). Experiments were performed in triplicate ($n = 3$). Isotherms were fitted using Guggenheim-Anderson-De Boer (GAB) model (Guggenheim 1966) through Eq. 1:

$$h(a_w) = \frac{Ncka_w}{[(1 + (c-1)ka_w)(1-ka_w)]} \tag{1}$$

where N is the monolayer water content (g of water per g of dried mass) related to primary binding sites of water molecules, c is a parameter related to the force of the water binding to monolayer, and k is a parameter related to the capability of water to bind to the multilayer (Salvay et al. 2003).

Water Vapor Permeability

Experimental water vapor permeability (P_w^{exp}) of films was measured using the cup method previously described (ASTM-E96 2016; Delgado et al. 2018b). Films were sealed on top of the cups containing a saturated solution of $BaCl_2$ that provides 90% r.h. Test cups were placed in desiccators maintained at a constant temperature of 22 °C and 10% r.h., provided by a saturated solution of NaOH. A fan was used to maintain uniform conditions inside the desiccators over the films

according to recommendations from previous authors (McHugh et al. 1993). Weight loss measurements were taken by weighing the test cup using an analytical balance ($\pm 10^{-3}$ g). Weight loss m versus time t was plotted and when the steady state (straight line) was reached 48 h further were registered. The experimental water vapor permeability P_w^{exp} was calculated according to Eq. 2:

$$P_w^{exp} = \frac{1}{A} \left(\frac{\Delta m}{\Delta t} \right) \frac{L}{\Delta p_w} \qquad (2)$$

where P_w^{exp} is given in units of g s^{-1} m^{-1} Pa^{-1}; A is the effective area of exposed film (2.2×10^{-3} m^2); ($\Delta m / \Delta t$) is the slope of a linear regression of weight loss versus time, L is the film thickness; $\Delta p_w = (p_{w2} - p_{w1})$ is the differential water vapor partial pressure across the film; and p_{w1} and p_{w2} are the partial pressures (Pa) of water vapor at the film surface outside and inside the cup, respectively, corrected by air gap distance (5×10^{-3} m in the present study) between the level of the saturated solution of BaCl$_2$ and the film position (Gennadios et al. 1994). Experiments were performed in triplicate ($n = 3$).

Antioxidant Activity of Kombucha Films

ABTS (2,29-azinobis-(3-ethylbenzothiazoline-6-sulfonic acid)) radical cation inhibition monitored by discoloration (Re et al. 1999) was used to study the antioxidant activity of K1 and K2 films. ABTS radical cation solution (ABTS$^{\bullet+}$) was produced by reacting 7 mM ABTS with 2.45 mM potassium persulfate (final concentration in water) and allowing the mixture to stand in the dark at room temperature for 16 h before use; this solution was called solution A. Afterwards, 1 ml of solution A was diluted in ethanol in order to obtain an absorbance of 0.70 ± 0.02 at 734 nm. This dilution of ABTS$^{\bullet+}$ was called solution B. Then, 10 mg of each film was placed in Eppendorf tubes and cover completely with 1 ml of solution B. The absorbance at 734 nm of the solution in contact with the film was measured at different times in order to record the discoloration if there was antioxidant activity of the sample. Therefore, antioxidant capacity was determined as the percentage of radical inhibition by the decrease in the absorbance at 734 nm and using Eq. 3:

%Radical Inhibition

$$= \frac{0.70 - \text{Sample Absorbance at 734 nm}}{0.70} \times 100 \qquad (3)$$

The percentage of radical inhibition of samples as function of time was fitted with a first order kinetics model, using a single exponential growth function as displayed in Eq. 4:

$$\%\text{Radical Inhibition } (t) = \%RI_\infty [1 - \exp(-t/\tau)] \qquad (4)$$

where $\%RI_\infty$ is the percentage of radical inhibition at equilibrium, and τ the rate constant of the process. Experiments were performed in triplicate ($n = 3$) at 22 °C.

Statistical Analyses

Statistical analyses were performed using OriginPro 8 (OriginLab Corporation). The data were subjected to the analysis of variance, and the means were compared by a post-hoc test (Tukey HSD). Differences were considered to be significant at $p < 0.05$.

Results and Discussion

The Visual Aspect and Quality Evaluation of Films

Kombucha films K1 and K2 were homogeneous, with no cracks, and presented a yellow-brownish color as seen in Fig. 1. K1 films (Fig. 1a) were clearer than K2 films (Fig. 1b); in addition, K2 films turned out to be more flexible than K1 films. This could be due to the presence of small molecules incorporated during the immersion of K2 disc in the fermentation broth, which obscure and plasticize the material. No differences were found in the visual aspect for all glycerol concentration. On the other hand, the gradual addition of plasticizer increased significantly the manual flexibility of the films. This is because glycerol locates between polymer chains, disrupting interpolymer bonds and spreading the chains apart increasing film flexibility (Gontard et al. 1993; Delgado et al. 2018a). The average thickness of all films studied was 0.100 ± 0.003 mm.

Film Microstructure

To observe film microstructure, micrographs of the faces and cross sections of unplasticized kombucha films K1 and K2 were obtained by scanning electron microscopy (SEM) (Fig. 2). Both unplasticized K1 and K2 films exhibited a continuous and homogeneous surfaces and cross sections, with no agglomerates, pores, faults, or film punctures (Fig. 2a and b). The cross section of unplasticized K2 film (Fig. 2b) exhibited rubber-like characteristics; this could be produced by a plasticized effect of small molecules incorporated during the immersion of the native disc in the fermentation broth. Regarding the surfaces of films, they also showed a continuous and homogenous matrix without pores (Fig. 2c and d). Surface observations revealed that the microstructure of both films was composed by a homogeneous and continuous matrix of ribbon-shaped nanofibers.

Fig. 1 Photographs of unplasticized kombucha films. **a** K1 film. **b** K2 film
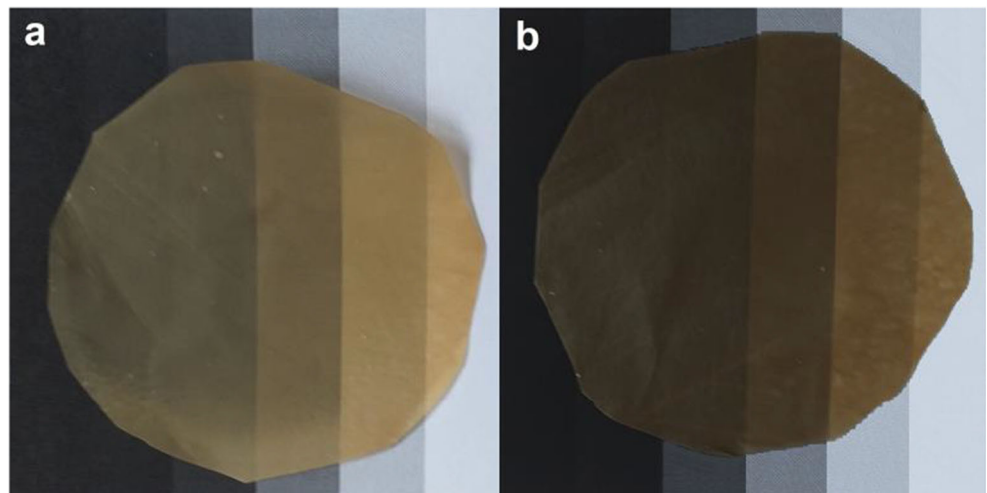
Infrared Spectroscopy of Films

Infrared spectra of unplasticized K1 and K2 films are shown in Fig. 3. The spectra have been normalized to the mayor peak at 1031 cm^{-1} for clarity. These spectra were very similar to those obtained previously for bacterial nanocellulose (Cerrutti et al. 2016), which is the main component of samples. In both spectra displayed in Fig. 3 could be identified a first absorption band in the region 3600–3000 cm^{-1} attributed to stretching vibration of hydroxyl groups (OH–) due to water and carbohydrates (Peltzer et al. 2018b; Coma et al. 2019).

The next absorption band in the 3000–2800 cm^{-1} zone was related to the symmetric and anti-symmetric stretching modes of C–H in methyl (CH$_3$) and methylene (CH$_2$) functional groups associated to cellulose (Li et al. 2009; Cerrutti et al. 2016).

In the range from 1800 to 1200 cm^{-1}, the band at 1641 cm^{-1} was assigned to polyphenols contribution (Wang et al. 2013) and also to the bending of O–H bonds in absorbed water molecules (Cerrutti et al. 2016; Coma et al. 2019). The peaks around 1428 cm^{-1} and 1340 cm^{-1} were observed in bacterial cellulose (Cerrutti et al. 2016). K1 film presented

Fig. 2 SEM microphotographs of kombucha films. **a** Cross section (× 800) of unplasticized K1 film. **b** Cross section (× 800) of unplasticized K2 film. **c** Surface (× 25,000) of unplasticized K1 film. **d** Surface (× 25,000) of unplasticized K2 film
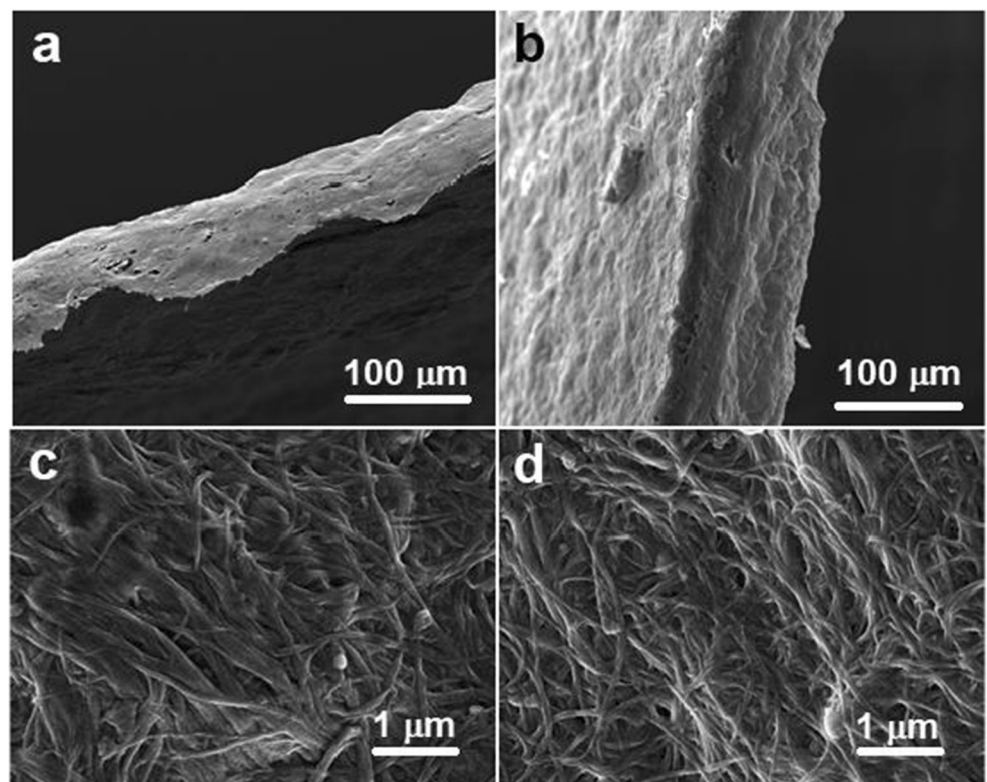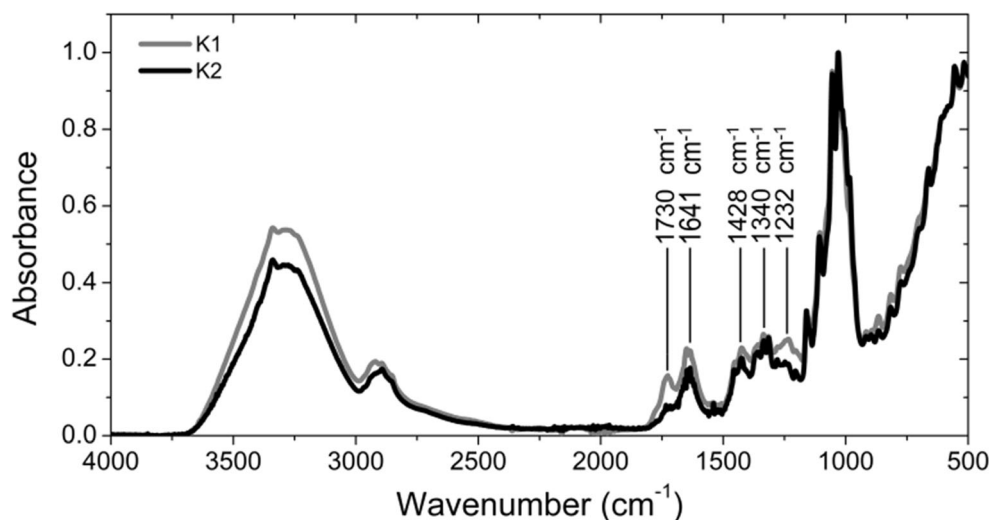
two distinctive peaks at 1730 cm^{-1} and 1232 cm^{-1}, corresponding to stretching of C=O and C–O–C of acetate groups, respectively (Song et al. 2012). The intensity of these two peaks was decreased in the spectra of K2 film. The presence of these peaks could be attributed to acetate compounds remaining in the samples after fermentation, which was mostly retained in the material coming from the floating disc. This is because in the floating disc are concentrated the acetic acid bacteria which synthesized both the cellulose disc and acetic acid, while the fermentation broth contains more yeasts producing alcohol which is oxidized by acetic acid bacteria (Gullo et al. 2018). Other authors indicated that in the region from 1800 to 1200 cm^{-1}, the presence of impurities, such as proteins, nucleic acids, and cells residues in the samples, contributes to the total absorbance and could overlap with cellulose bands in that region (Fuller et al. 2018).

The spectra of K1 and K2 films revealed a main absorption band in the 1200–940 cm^{-1} region which holds the peaks mainly assigned to stretching modes of carbohydrate macromolecules and side groups (C–O–C, C–OH, C–H). In kombucha films K1 and K2, the peaks in this region were associated with the vibrational modes of glucose from cellulose structure (Li et al. 2009; Cerrutti et al. 2016; Song et al. 2012).

Thermogravimetric Analysis of Films

Thermogravimetric analysis of K1 and K2 films are shown in Fig. 4. Figure 4a shows the weight loss of unplasticized K1 and K2 films that were previously hydrated in equilibrium in an atmosphere at 90% r.h. Weight loss up to 100 °C was attributed to water evaporation or dehydration. As seen in Fig. 4b, percentage of retained water values was lower in the K2 sample, indicating that the force of the water binding to the matrix was weaker than in the sample K1. Following the

dehydration zone shown in Fig. 4a, weight loss was due to thermal degradation of molecules and macromolecules.

Figure 4c and d show the weight loss of dried K1 and K2 films with different content of glycerol. Figure 4e and f display the respective derivatives of weight loss with respect to temperature. Thermogravimetric analyses of dehydrated samples K1 and K2 showed a multistep thermal degradation profile with four different degradation zones. First degradation zone from 100 to 130 °C was related to low molecular weight molecules degradation. The second zone from 130 to 290 °C involves the degradation of glycerol (Arrieta et al. 2013), tannins, and phenolic compounds (Xia et al. 2015), in addition to degradation of phospholipids, nucleic acids, and cell residues (Delgado et al. 2018a), as well as degradation of proteins remaining in the samples (Guerrero et al. 2010). Zones I and II involved weight loss of 32% and 35% of the total dry mass of unplasticized samples K1 and K2, respectively.

The third zone from 290 to 390 °C presented in both samples K1 and K2 a maximum degradation rate at 350 ± 3 °C which was attributed to thermal degradation of bacterial cellulose (Barud et al. 2011; Cerrutti et al. 2016). Finally, after 390 °C starts the last zone which has formerly been attributed to the degradation of polymeric chains and the six-member cyclic structure, pyran, distinguishing it from the previous decomposition step assigned to the removal of molecular fragments such as hydroxyl and hydroxymethyl groups (Cheng et al. 2009; Cerrutti et al. 2016). Weight loss registered in zones III and IV for unplasticized samples K1 and K2 was 43% and 40%, respectively.

It is seen in Fig. 4c and d an effect due to the plasticization of the matrix favoring thermal degradation in both samples. This is due to the presence of glycerol in the film matrix, which increased chain mobility and exposed polymer chains even more to the thermal degradation (Coma et al. 2019). This effect was more important in sample K2 with 30 wt%

Fig. 4 Thermogravimetric analysis of kombucha films. **a** Mass loss of unplasticized films K1 and K2 previously hydrated at 90% r.h. **b** Percentage of retained water of unplasticized films K1 and K2 previously hydrated at 90% r.h. **c** Mass loss of dried films K1 with different content of glycerol. **d** Mass loss of dried films K2 with different content of glycerol. **e** Derivative of mass loss of dried films K1. **f** Derivative of mass loss of dried films K2
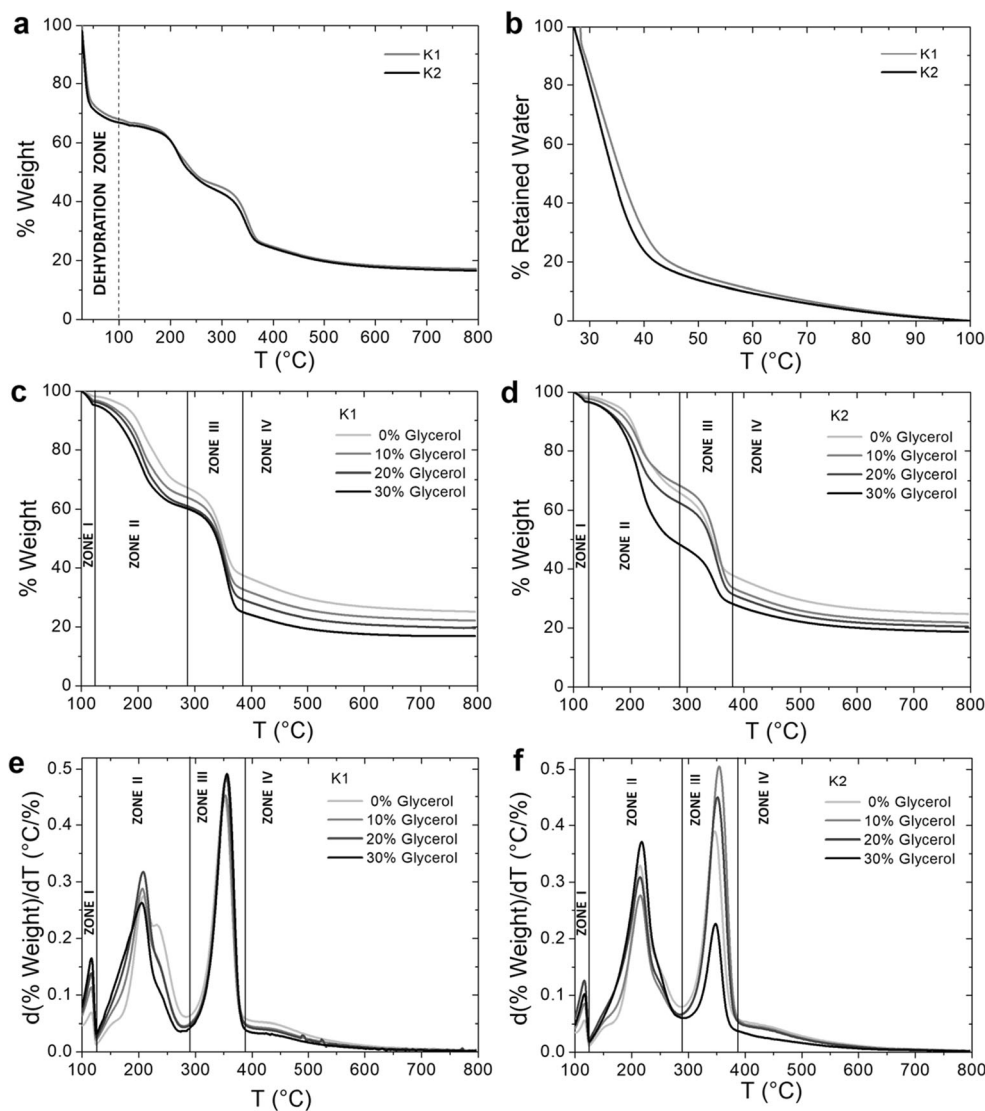
glycerol. The final residue at 800 °C was affected by the initial quantity of glycerol added to samples (Fig. 4c and d).

Differential Scanning Calorimetry

Glass transition temperatures (T_g) of kombucha films and the effect of glycerol and moisture content were studied by DSC experiments. The determination of T_g is relevant because it greatly affects the thermomechanical properties and physical and chemical stabilities of the material (Matveev et al. 2000). In Fig. 5 are shown DSC thermograms of kombucha films K1 and K2.

The effect of glycerol content on the T_g of samples was studied in dry conditions in order to observe thermal events independently to the water content of films that could also plasticize the matrix. As it is seen in Fig. 5a and b, films without glycerol presented the highest T_g; then, the T_g decreased with increased glycerol concentration due to the

plasticization process. The unplasticized sample K1 presented the T_g at 16 ± 1 °C, and samples with 10, 20, and 30 wt% glycerol revealed T_gs at -13 ± 1, -36 ± 2, and -51 ± 2 °C, respectively (Fig. 5a). Moreover, the unplasticized sample K2 presented the T_g at 3 ± 1 °C and samples with 10, 20, and 30 wt% glycerol exhibited T_gs at -16 ± 2, -42 ± 2, and -55 ± 1 °C, respectively (Fig. 5b). This behavior agrees with other studies on the effect of glycerol concentration on T_g values of biopolymeric films (Delgado et al. 2018a; Coma et al. 2019). The decrease of T_g with the addition of plasticizer may be explained by theoretical approaches such as free volume or classical thermodynamic theories as proposed by Couchman and Karaz (1978). In addition, the plasticizer reduces the attractive forces between polymer chains, producing an increase in the molecular space and mobility favoring the transition from glassy to rubbery state. It was observed that at the same level of glycerol content, K2 samples exhibited lower T_gs than K1 samples. This could be understood considering

Fig. 5 DSC thermograms of kombucha films. **a** Dried K1 films with different content of glycerol. **b** Dried K2 films with different content of glycerol. **c** Unplasticized K1 films previously hydrated at 0, 52, 75, and 90% r.h. **d** Unplasticized K2 films previously hydrated at 0, 52, 75, and 90% r.h
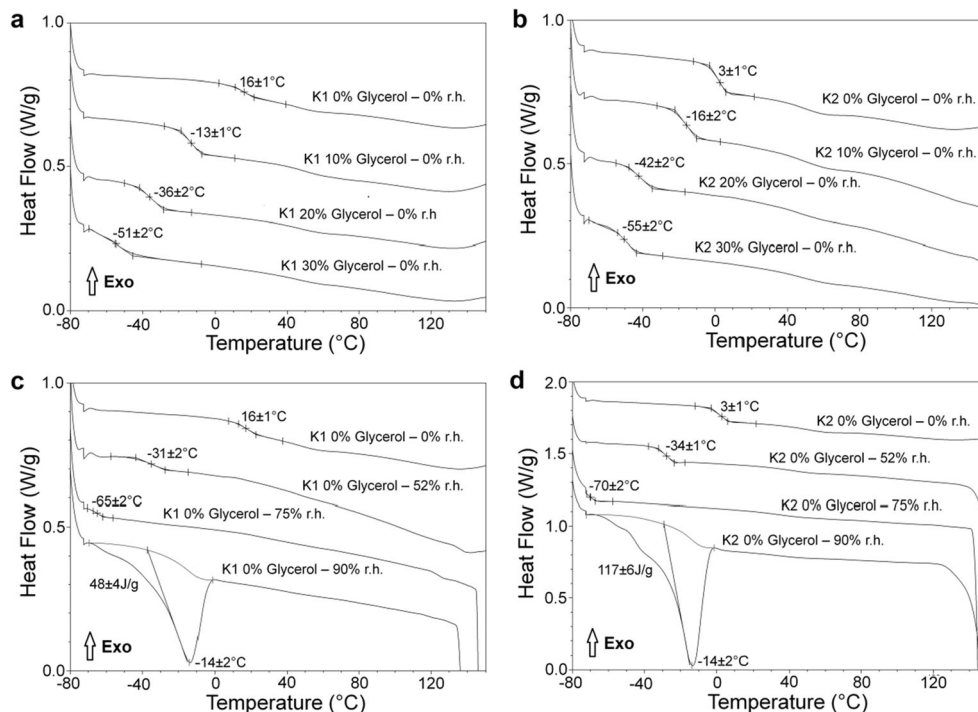
that K2 samples had an additional plasticization provided by substances incorporated during the 21 days of immersion of the native disc in the fermentation broth.

The effect of hydration water on the T_g was studied in unplasticized samples in order to observe thermal events independently to the glycerol content of films. Figure 5c and d show the effect of water in the polymer matrices K1 and K2 by the hydration of samples at different r.h. It was observed that T_g decreased with the increase in hydration water of the unplasticized films, as expected. The obtained T_g values for sample K1 were 16 ± 1, -31 ± 2, and -65 ± 2 °C for films previously hydrated at 0, 52, and 75% r.h., respectively (Fig. 5c), while sample K2 presented T_gs at 3 ± 1, -34 ± 1, and -70 ± 2 °C for films previously hydrated at 0, 52, and 75% r.h., respectively (Fig. 5d). As follows, hydration water acts as a plasticizer and films acquired more rubber-like characteristics as hydration increases. The plasticizing effect of water on proteins, polysaccharides, and their mixtures was already observed by other authors (Matveev et al. 2000; Coma et al. 2019). Samples that were hydrated at 90% r.h. exhibited a significant endotherm that was related to the latent heat of fusion of frozen water in samples. At this condition of hydration, T_g did not appear visible because the change in heat flow associated with the glass transition was practically negligible as compared to the latent heat of fusion. In addition, it is possible that the T_gs of these samples had temperature values lower to the limit analyzed.

These results indicated that in laboratory conditions (22 °C and 52% r.h.), all samples had rubber-like characteristics and constituted flexible materials.

Mechanical Properties

Uniaxial tensile tests of kombucha films K1 and K2 with different glycerol contents were performed at room experimental conditions of 22 °C and 52% r.h. The tensile parameters Young's modulus Y (MPa), maximum tensile strength TS_{max} (MPa), and deformation at break e (%) were calculated from the experimental stress–strain curves (Fig. 6) and are shown in Table 1. It was observed in both samples K1 and K2 a decrease in Y and TS_{max} with the addition of glycerol, whereas e (%) was increased. Parameter Y is related to the intensity of intermolecular bonds in the matrix while TS_{max} is associated to the number of intermolecular bonds (Smith 1997). This behavior showed how the plasticizer works at the molecular level producing changes in the spacing between molecules, decreasing interpolymer interactions, and allowing greater mobility. This increased capability of movement, resulted macroscopically in rubber-like characteristic state with greater flexibility and extensibility (Delgado et al. 2018a). The significant decrease in the Young's modulus with plasticization was not accompanied by important increase in the deformation at break value e (%). An important increase of e (%) was observed in other polysaccharide-based matrices, such as water kefir films, where the addition of 30 wt% glycerol increases from 2.5 ± 0.2 to 275 ± 15% (Coma et al. 2019).

K1 and K2 films presented an identical behavior of mechanical parameters with the addition of glycerol (Fig. 6; Table 1). However, K1 films presented Y and TS_{max} values higher than those corresponding to K2 film at the same level of glycerol content. As observed in Table 1, unplasticized K1

Fig. 6 Representative stress–strain curves for one of ten replications of the mechanical test performed for kombucha films with different content of glycerol. **a** K1 films. **b** K2 films. Young's modulus Y was calculated from the slope in the linear region, maximum tensile strength TS_{max} from the maximum value of the nominal stress and deformation at break e (%) from the maximum value of the nominal strain
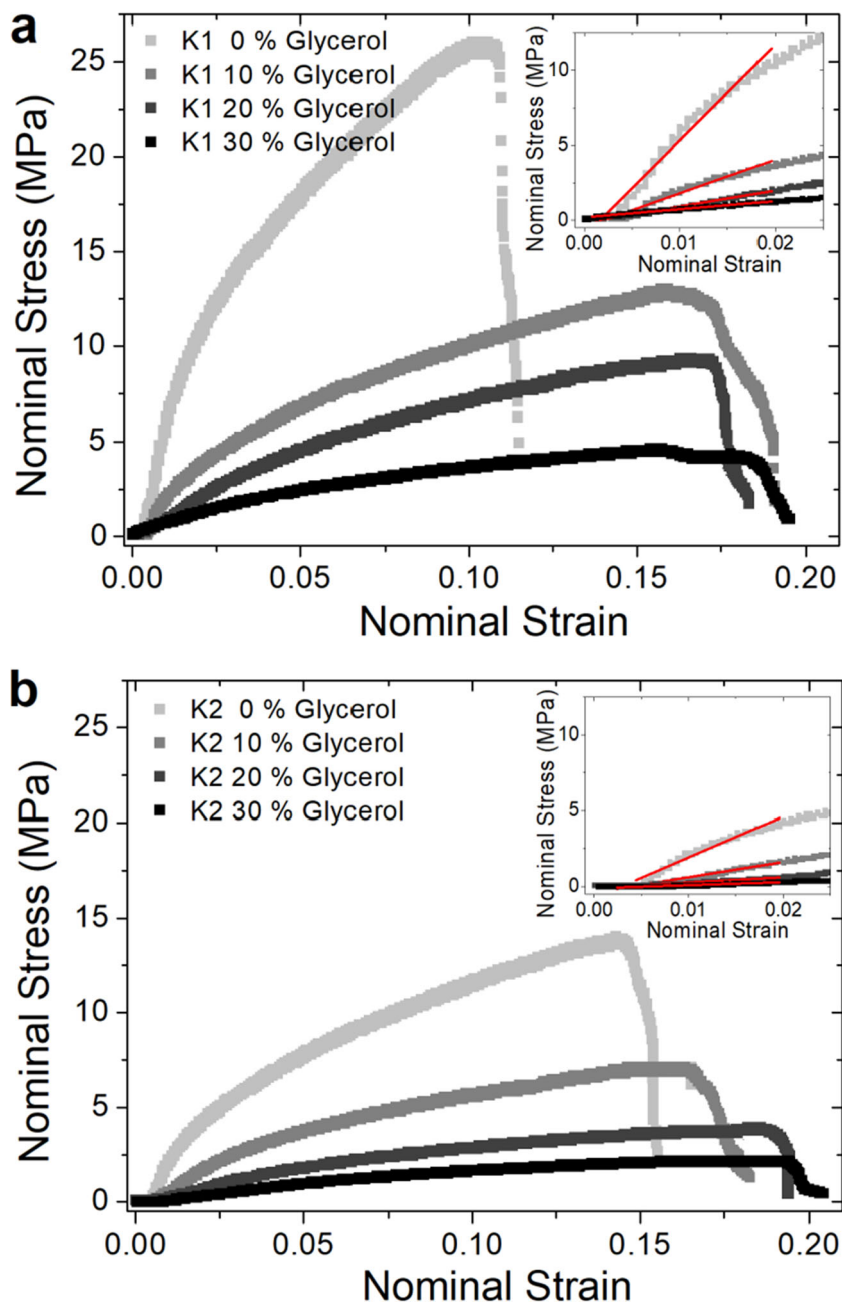
film presented a value of Y of 723 ± 97 MPa and a value of TS_{max} of 25 ± 2 MPa, which were larger than respective values of 262 ± 31 MPa and 13 ± 2 MPa of unplasticized K2 film. Another interesting point, shown in Table 1, is that K1 films plasticized with 10 wt% glycerol presented similar values of Y, TS_{max}, and e(%) that obtained for unplasticized K2 film, considering experimental errors. According to the mechanical performance, it was evidenced that the unplasticized K2 film had an intrinsic plasticization comparable with K1 films plasticized with 10% glycerol. This intrinsic plasticization was given by the substances incorporated during the immersion of native disc in the fermentation broth. This could be an advantage for film development since it is possible to avoid the addition of plasticizers representing a reduction in the cost of film formulation or drawbacks that plasticizer may represents.

Unplasticized K1 and K2 films presented higher values of Y as compared with unplasticized films based on polysaccharides and proteins such as starch, alginate, pea protein, and gluten (Jost and Stramm 2016). Moreover, unplasticized films based on yeast cell wall containing basically β-glucan (Peltzer et al. 2018b) presented similar values of Y as compared with unplasticized K1 films.

Table 1 Mechanical parameters of K1 and K2 films with different contents of glycerol. The mean and standard deviation ($n = 10$) are reported. The same letters in the data reported in a column mean non-significant differences ($p < 0.05$)

Formulation	Y (MPa)	TS_{max} (MPa)	e (%)
K1 0% glycerol	723 ± 97a	25 ± 2a	12 ± 1c
K1 10% glycerol	253 ± 24b	13 ± 1b	17 ± 2ab
K1 20% glycerol	90 ± 10d	9 ± 1c	18 ± 2ab
K1 30% glycerol	52 ± 6d	4 ± 1d	19 ± 2a
K2 0% glycerol	262 ± 31b	13 ± 2b	15 ± 1b
K2 10% glycerol	116 ± 12c	7 ± 1c	17 ± 2ab
K2 20% glycerol	41 ± 3e	3.6 ± 0.4d	19 ± 2a
K2 30% glycerol	30 ± 3f	2.4 ± 0.4e	20 ± 2a

It was reported elastic modulus Y values of 167 GPa for the native cellulose I crystal regions (Tashiro and Kobayashi 1991) and of 143 GPa for highly crystalline tunicate cellulose whiskers (Šturcová et al. 2005). These values were considerably higher than elastic modulus values of unplasticized K1 and K2 films. Cellulose fibrils consist of different hierarchical microstructures commonly known as nanosized fibrils, which are a combination of a crystalline and amorphous region (Cho and Park 2011). Isolation of crystalline cellulosic regions is generally realized by an acid hydrolysis (Dufresne 2017). In the crystalline regions, cellulose chains are stabilized laterally by a hydrogen bonds network between hydroxyl groups increasing structural strength and stiffness (Cho and Park 2011). In K1 and K2 films which contained native cellulose, the microstructure was composed by ribbon-shaped nanofibers containing crystalline and amorphous region. The existence of amorphous regions, the presence of other components from the culture medium, as well the sonication applied which might produce short-length polymer chains could have been able to reduce significantly the average strength of the intermolecular bonds decreasing Y modulus.

Hydration and Water Vapor Transport Properties

Water sorption isotherms of K1 and K2 films at 0, 10, 20, and 30 wt% of glycerol are shown in Fig. 7a and b, respectively, and experimental points were fitted with GAB model done by Eq. 1. It was observed that the addition of glycerol increased the amount of hydration water, preserving the shape of the isotherms. This behavior was also detected in films based on polysaccharides (Mali et al. 2005); proteins (Coupland et al. 2000); and natural multicomponent films such as yeast cell wall (Peltzer et al. 2018b), integral yeast biomass (Delgado et al. 2018a), and integral water kefir grains biomass (Coma et al. 2019). In general, hydrophilic films made from biopolymers present water sorption isotherms with a slight increase in hydration water content at low values of a_w and a sharp
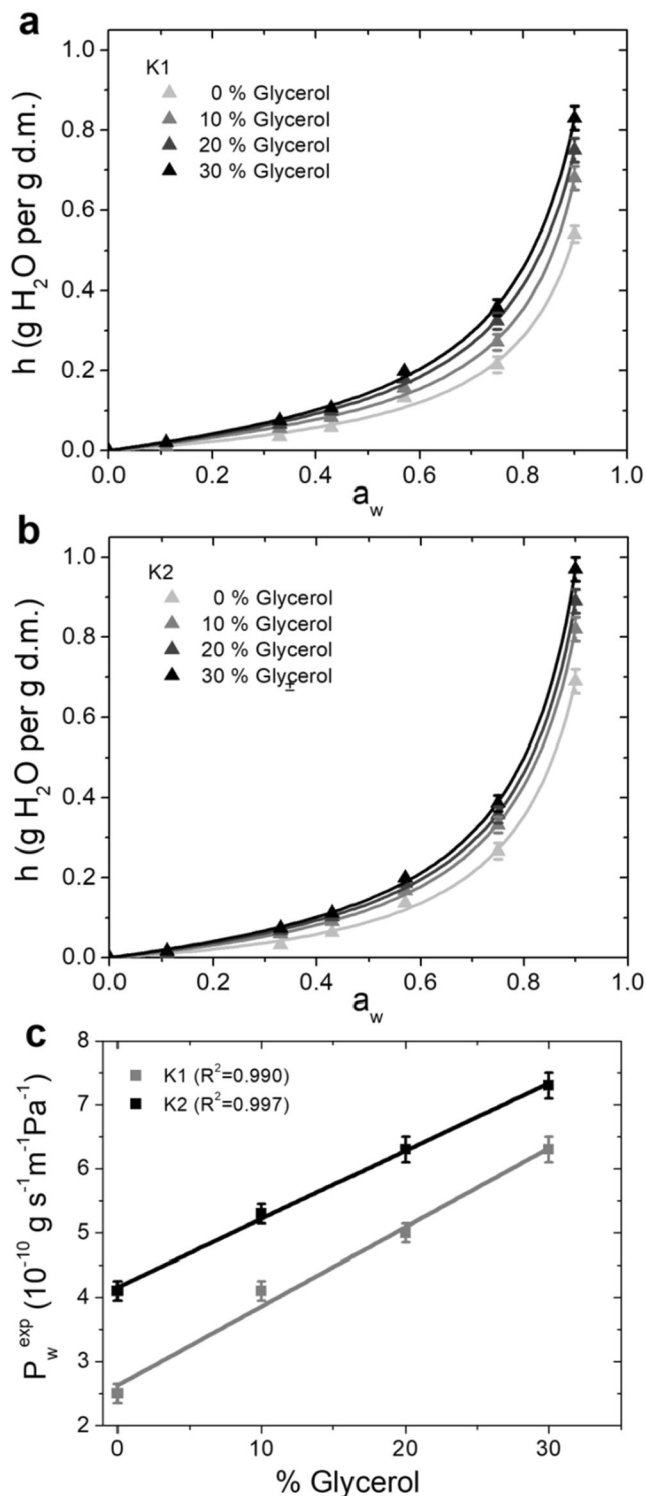

Fig. 7 Hydration and water vapor permeability of kombucha films. **a** Water sorption isotherms of kombucha K1 films with different content of glycerol. **b** Water sorption isotherms of kombucha K2 films with different content of glycerol. Experimental data was fitted with Eq. 1 and showed in Table 2. **c** Experimental water vapor permeability P_w^{exp} of K1 and K2 films as a function of the content of glycerol

increase for $a_w > 0.6$ (Peltzer et al. 2017). This shape of sorption isotherms suggested the existence of a small amount of

water directly bound to the polymeric matrix, forming the monolayer (Delgado et al. 2016). Then, most of the hydration water was forming multilayers and was indirectly bound to the polymeric matrix (Salvay et al. 2003). Therefore, hydration water in hydrophilic biopolymeric materials is susceptible to be moved by diffusion mechanism (Delgado et al. 2018b).

Comparing the isotherm of unplasticized K1 films displayed in Fig. 7a with isotherms of other unplasticized biopolymeric films, it could be observed a similar hydration in starch films (Bertuzzi et al. 2007) and myofibrillar protein films (Cuq et al. 1997). However, hydration of unplasticized K1 films was higher than the hydration of films based on yeast cell wall (Peltzer et al. 2018b), whole yeast biomass (Delgado et al. 2016), and water kefir films (Coma et al. 2019). On the other hand, it could be appreciated, comparing Fig. 7a and b, that K1 film presented lower hydration values than those corresponding to K2 film at the same level of glycerol content.

Table 2 displays the parameters obtained from fitting sorption isotherms with the GAB model. In both K1 and K2 films parameter N related to the number of primary binding sites of hydration increased with the glycerol content, while parameter c linked to the force of the water binding to these primary sites and parameter k related to the capability of water to be bounded to the multilayer were independent of glycerol content. As follows, the hydration equilibrium value at 90% r.h. ($h_{90\%r.h.}$) was increased with the glycerol content. Glycerol interacted with cellulose chains by establishing hydrogen bonds with the reactive groups of polymer. Therefore, glycerol incorporated to the film matrix decreased the attractive forces between polymer chains and increased free volume and segmental motions, producing a global increase in hydration water content.

It is seen in Table 2 that unplasticized K1 film presented a value of $h_{90\%r.h.}$ of 0.54 ± 0.02 g H_2O per g d.m., which was smaller than corresponding value of $h_{90\%r.h.}$ of 0.69 ± 0.02 g H_2O per g d.m. measured for unplasticized K2 film. Moreover, K1 film plasticized with 10 wt% glycerol presented identical values of $h_{90\%r.h.}$ than that measured for unplasticized K2 film, considering experimental errors. This suggested again that the unplasticized K2 film had an intrinsic plasticization that increased the hydration. This intrinsic

plasticization, provided by substances incorporated during the immersion of the native disc in the fermentation broth, decreased around 30% the parameter c values. Therefore, the force of the water binding to K2 films was weaker than in K1 films. In this way, the intrinsic plasticization produces a global increase in hydration water content, allowing greater mobility to water molecules in K2 films, as also described thermogravimetric analyses.

Hydration water affects the main structural and functional properties of hydrophilic films, because water acts as plasticizer by embedding itself between the polymer chains, spacing them, lowering the glass transition temperature T_g, and affecting flexibility. Moreover, hydration water is related with the water vapor transport properties through hydrophilic polymeric films. It was found from micrographs of Fig. 2 that K1 and K2 films exhibited a continuous and homogenous matrix, without pores, faults, or film punctures. These studies indicated that the water transport in K1 and K2 films did not occur through pores but by means of the mechanism of sorption-diffusion-desorption (Roy et al. 2000). Therefore, water vapor permeability depends on the hydration or water solubility in the film as well as the mobility of water in the matrix (Delgado et al. 2018b).

Experimental water vapor permeability P_w^{exp} of K1 and K2 films at 0, 10, 20, and 30 wt% of glycerol was obtained by Eq. 2 and is shown in Fig. 7c. In both samples, it was detected that P_w^{exp} increased linearly with the glycerol content in the film. A linear relation between permeability and glycerol content was also observed in other biodegradable matrices such as water kefir grain biomass–based films (Coma et al. 2019), yeast biomass–based films (Delgado et al. 2018b), yeast cell wall films (Peltzer et al. 2018b), and starch films (Bertuzzi et al. 2007). The effect of glycerol increasing water vapor permeability was observed in the most of protein-based films and polysaccharide-based films (Delgado et al. 2018b). Water sorption isotherms of K1 and K2 films revealed that the increase in the amount of glycerol in the film produced a global increase in hydration. Consequently, it was expected that water vapor permeability of kombucha films would be increased with the raising percentage of glycerol. On the other

Table 2 Values of the GAB parameters fitted for the water sorption isotherms of K1 and K2 films displayed in Fig. 7a and b, respectively. $h_{90\%r.h.}$ refers to the hydration equilibrium value at 90% r.h. The reported values of the statistical parameter R^2 indicate a very good acceptance of the fit model. Errors are estimated from the fit analysis

Formulation	$h_{90\%r.h.}$ (g H_2O/g)	N (g H_2O/g)	c	k	R^2
K1 0% glycerol	0.54 ± 0.02	0.07 ± 0.01	1.5 ± 0.2	0.95 ± 0.02	0.997
K1 10% glycerol	0.68 ± 0.02	0.09 ± 0.01	1.5 ± 0.2	0.96 ± 0.01	0.998
K1 20% glycerol	0.75 ± 0.03	0.12 ± 0.01	1.6 ± 0.3	0.96 ± 0.01	0.999
K1 30% glycerol	0.83 ± 0.03	0.13 ± 0.01	1.6 ± 0.3	0.96 ± 0.01	0.999
K2 0% glycerol	0.69 ± 0.02	0.10 ± 0.01	1.0 ± 0.1	0.96 ± 0.01	0.998
K2 10% glycerol	0.82 ± 0.03	0.12 ± 0.01	1.0 ± 0.2	0.96 ± 0.01	0.999
K2 20% glycerol	0.89 ± 0.03	0.14 ± 0.01	1.1 ± 0.2	0.97 ± 0.02	0.997
K2 30% glycerol	0.97 ± 0.03	0.15 ± 0.01	1.1 ± 0.3	0.97 ± 0.01	0.999
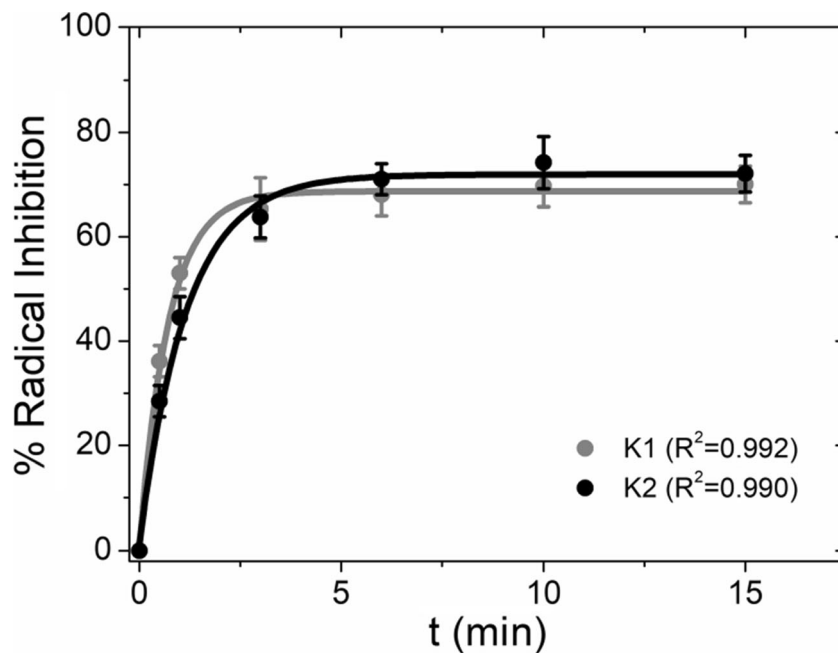
hand, K2 films presented P_w^{exp} values higher than those corresponding to K1 film at the same level of glycerol content. Moreover, K1 film plasticized with 10 wt% glycerol presented similar values of P_w^{exp} that the measured for unplasticized K2 film. This is because of the intrinsic plasticization of K2 that produces a global increase in hydration and the mobility of water molecules, raising permeability with respect to K1 films.

Water vapor permeability of biopolymer-based films is an important property, indicating their ability to control water vapor transport between a system of interest and its surroundings. Comparison of water vapor permeability values of hydrophilic polymeric films is difficult because of non-ideal behavior that occurs in matrices interacting with permeant water, especially the strong dependence of permeability coefficient with film thickness and the differential water vapor partial pressure across the test Δp_w. Nevertheless, the order of magnitude of the measured P_w^{exp} for K1 and K2 films was similar to films obtained from other biopolymers.

Antioxidant Activity

Antioxidant activity of unplasticized K1 and K2 films was determined by ABTS method and expressed as percent of radical inhibition using Eq. 3. Figure 8 shows the kinetics of the percent of radical inhibition of samples K1 and K2. The curves connecting the experimental data were the best fitted using the exponential growth function given in Eq. 4 and showed that radical inhibition followed a first order kinetics. The rate constant parameter τ obtained from the fit was 0.7 ± 0.1 min for K1 sample and 1.2 ± 0.1 min form K2 sample and revealed that the radical inhibition process carried out by K1

film was faster than the inhibition performed by K2 film. However, the percentage of radical inhibition at equilibrium $\%RI_\infty$ achieved for K1 film was $69 \pm 2\%$ and $72 \pm 2\%$ for K2 film. These values of $\%RI_\infty$ indicated an important antioxidant capacity of both K1 and K2 films, clearly superior to whey protein isolate–based films containing free and nanoencapsulated *Thymus vulgaris* extract (Aziz and Almasi 2018) and gelatin-based films incorporated with papaya peel microparticles (de Moraes Crizel et al. 2018).

The antioxidant activities of K1 and K2 samples could be due to the presence of organic acids and bioactive phenolic compounds in the matrix film that could be incorporated from the culture medium (Dima et al. 2017). Natural molecules from the culture medium of kombucha represent a heterogeneous mixture of negatively charged, nitrogen-containing, phenols and polyphenols, glucuronic acid, D-saccharic acid-1.4-lactone, and B-vitamin complex (Dima et al. 2017). The antioxidant activity of K1 and K2 films was comparable to the high percentage of radical inhibition measured for Fish gelatin films incorporated with β-cyclodextrin/curcumin complexes (Wu et al. 2018) and low-density polyethylene films containing 15% sodium ascorbate (Sangatash et al. 2016).

Conclusions

In this work, new biodegradable and active materials were developed using the integral by-product produced during fermentation of kombucha tea. The films obtained were flexible and exhibited a great continuity and homogeneity with the microstructure composed by a homogeneous and continuous cellulosic matrix of ribbon-shaped nanofibers. Infrared

spectroscopy, thermogravimetric analyses, and antioxidant capacity assays indicated that samples were constituted basically by cellulose with the presence of low and high molecular weight compounds which presented high antioxidant activity, suggesting that the materials are natural active systems. A natural plasticization was observed and is an advantage regarding decrease or elimination of plasticizers reducing the cost of film formulation in addition to the incorporation of bioactive molecules with functional and beneficial properties. The new approach to develop materials presented in this work contributes to a more efficient process with less waste and allows exploiting the properties of whole biomass of the cellulosic by-product, e.g., an important antioxidant activity. The results obtained demonstrated the potential of the whole biomass to be used in the development of food contact materials. Now efforts should be directed to obtain these active materials to an industrial level.

Compliance with Ethical Standards

Conflict of Interest   The authors declare that they have no conflict of interest.

References

Arrieta, M. P., Peltzer, M. A., Garrigós, M. C., & Jiménez, A. (2013). Structure and mechanical properties of sodium and calcium caseinate edible active films with carvacrol. *Journal of Food Engineering, 114*(4), 486–494.

ASTM D882-97. (1997). Standard test method for tensile properties of thin plastic sheeting. In *Annual book of ASTM standards*. Philadelphia: American Society for Testing and Materials.

ASTM-E96. (2016). *Standard test methods for water vapor transmission of materials*. ASTM International: West Conshohocken.

Aziz, S. G., & Almasi, H. (2018). Physical characteristics, release properties, and antioxidant and antimicrobial activities of whey protein isolate films incorporated with thyme (*Thymus vulgaris* L.) extract-loaded nanoliposomes. *Food and Bioprocess Technology, 11*(8), 1552–1565.

Barud, H. S., Ribeiro, C. A., Capela, J. M. V., Ribeiro, S. J. L., & Messadeq, Y. (2011). Kinetic parameters for thermal decomposition of microcrystalline, vegetal, and bacterial cellulose. *Journal of Thermal Analysis and Calorimetry, 105*(2), 421–426.

Bertuzzi, M. A., Castro Vidaurre, E. F., Armada, M., & Gottifredi, J. C. (2007). Water vapor permeability of edible starch based films. *Journal of Food Engineering, 80*(3), 972–978.

Cazón, P., Velazquez, G., Ramírez, J. A., & Vázquez, M. (2017). Polysaccharide-based films and coatings for food packaging: a review. *Food Hydrocolloids, 68*, 136–148.

Cerrutti, P., Roldán, P., García, R. M., Galvagno, M. A., Vázquez, A., & Foresti, M. L. (2016). Production of bacterial nanocellulose from wine industry residues: importance of fermentation time on pellicle characteristics. *Journal of Applied Polymer Science, 133*, 43109.

Cheng, K.-C., Catchmark, J. M., & Demirci, A. (2009). Effect of different additives on bacterial cellulose production by Acetobacter xylinum and analysis of material property. *Cellulose, 16*(6), 1033–1045.

Cho, M.-J., & Park, B.-D. (2011). Tensile and thermal properties of nanocellulose-reinforced poly(vinyl alcohol) nanocomposites. *Journal of Industrial and Engineering Chemistry, 17*(1), 36–40.

Coma, M. E., Peltzer, M. A., Delgado, J. F., & Salvay, A. G. (2019). Water kefir grains as an innovative source of materials: study of plasticiser content on film properties. *European Polymer Journal, 120*, 109234.

Cottet, C., Ramírez Tapias, Y. A., Delgado, J. F., de la Osa, O., Salvay, A. G., & Peltzer, M. A. (2020). Biobased materials from microbial biomass and its derivatives. *Materials, 13*(6), 1263.

Couchman, P. R., & Karaz, F. E. (1978). A classical thermodynamic discussion of the effect of composition on glass-transition temperature. *Macromolecules, 11*, 177–188.

Coupland, J. N., Shaw, N. B., Monahan, F. J., O'Riordan, E. D., & O'Sullivan, M. (2000). Modeling the effect of glycerol on the moisture sorption behavior of whey protein edible films. *Journal of Food Engineering, 43*(1), 25–30.

Cuq, B., Gontard, N., Aymard, C., & Guilbert, S. (1997). Relative humidity and temperature effects on mechanical and water vapor barrier properties of myofibrillar protein-based films. *Polymer Gels and Networks, 5*(1), 1–15.

de Moraes Crizel, T., de Oliveira Rios, A., Alves, D. V., Bandarra, N., Moldão-Martins, M., & Hickmann Flôres, S. (2018). Biodegradable films based on gelatin and papaya peel microparticles with antioxidant properties. *Food and Bioprocess Technology, 11*(3), 536–550.

Delgado, J. F., Sceni, P., Peltzer, M. A., Salvay, A. G., de la Osa, O., & Wagner, J. R. (2016). Development of innovative biodegradable films based on biomass of Saccharomyces cerevisiae. *Innovative Food Science & Emerging Technologies, 36*, 83–91.

Delgado, J. F., Peltzer, M. A., Salvay, A. G., de la Osa, O., & Wagner, J. R. (2018a). Characterization of thermal, mechanical and hydration properties of novel films based on Saccharomyces cerevisiae biomass. *Innovative Food Science & Emerging Technologies, 48*, 240–247.

Delgado, J. F., Peltzer, M. A., Wagner, J. R., & Salvay, A. G. (2018b). Hydration and water vapour transport properties in yeast biomass based films: a study of plasticiser content and thickness effects. *European Polymer Journal, 99*, 9–17.

Dima, S. O., Panaitescu, D. M., Orban, C., Ghiurea, M., Doncea, S. M., Fierascu, R. C., et al. (2017). Bacterial nanocellulose from side-streams of kombucha beverages production: Preparation and physical-chemical properties. *Polymers, 9*, 5–10.

Dourado, F., Ryngajllo, M., Jedrzejczak-Krzepkowska, M., Bielecki, S., & Gama, F. M. (2016). Taxonomic review and microbial ecology in bacterial nanocellulose fermentation. In M. Gama, F. Dourado, & S. Bielecki (Eds.), *Bacterial nanocellulose: from biotechnology to bioeconomy* (pp. 1–17). Elsevier B.V.

Dufresne, A. (2017). Cellulose nanomaterial reinforced polymer nanocomposites. *Current Opinion in Colloid & Interface Science, 29*, 1–8.

Dutta, H., & Paul, S. K. (2019). Kombucha drink: production, quality, and safety aspects. In *Production and Management of Beverages* (pp. 259–288). Woodhead Publishing.

Fuller, M. E., Andaya, C., & McClay, K. (2018). Evaluation of ATR-FTIR for analysis of bacterial cellulose impurities. *Journal of Microbiological Methods, 144*, 145–151.

Gennadios, A., Weller, C. L., & Gooding, C. H. (1994). Measurement errors in water vapor permeability of highly permeable, hydrophilic edible films. *Journal of Food Engineering, 21*(4), 395–409.

Gontard, N., Guilbert, S., & Cuq, J.-L. (1993). Water and glycerol as plasticizers affect mechanical and water vapor barrier properties of an edible wheat gluten film. *Journal of Food Science, 58*(1), 206–211.

Grand View Research (2020). Kombucha market size, share & trends analysis report by flavor (original, flavored), by distribution channel (supermarkets, health stores, online stores), by region, and segment forecasts, 2020–2027. Retrieved from https://www.grandviewresearch.com/industry-analysis/kombucha-market. Accessed 18 May 2020.

Guerrero, P., Retegi, A., Gabilondo, A., & de la Caba, K. (2010). Mechanical and thermal properties of soy protein films processed by casting and compression. *Journal of Food Engineering, 100*(1), 145–151.

Guggenheim, E. A. (1966). *Applications of statistical mechanics* (pp. 186–206). Oxford: Claredon Press.

Gullo, M., La China, S., Falcone, P. M., & Giudici, P. (2018). Biotechnological production of cellulose by acetic acid bacteria: current state and perspectives. *Applied Microbiology and Biotechnology, 102*(16), 6885–6898.

Jayabalan, R., Malbaša, R. V., Lončar, E. S., Vitas, J. S., & Sathishkumar, M. (2014). A review on kombucha tea-microbiology, composition, fermentation, beneficial effects, toxicity, and tea fungus. *Comprehensive Reviews in Food Science and Food Safety, 13*(4), 538–550.

Johansson, C., Bras, J., Mondragon, I., Nechita, P., Plackett, D., Šimon, P., et al. (2012). Renewable fibers and bio-based materials for packaging applications - a review of recent developments. *BioResources, 7*, 2506–2552.

Jost, V., & Stramm, C. (2016). Influence of plasticizers on the mechanical and barrier properties of cast biopolymer films. *Journal of Applied Polymer Science, 133*, 42513.

Kim, J., & Adhikari, K. (2020). Current trends in kombucha: marketing perspectives and the need for improved sensory research. *Beverages, 6*(1), 15.

Li, M., & Ye, R. (2017). Edible active packaging for food application: materials and technology. In M. A. Masuelli (Ed.), *Biopackaging* (1st ed., p. 1). Boca Raton: CRC Press.

Li, J., Zhang, L.-P., Peng, F., Bian, J., Yuan, T.-Q., Xu, F., & Sun, R.-C. (2009). Microwave-assisted solvent-free acetylation of cellulose with acetic anhydride in the presence of iodine as a catalyst. *Molecules, 14*(9), 3551–3566.

Li, M., Zhang, F., Liu, Z., Guo, X., Wu, Q., & Qiao, L. (2018). Controlled release system by active gelatin film incorporated with β-cyclodextrin-thymol inclusion complexes. *Food and Bioprocess Technology, 11*(9), 1695–1702.

Mali, S., Sakanaka, L. S., Yamashita, F., & Grossmann, M. V. E. (2005). Water sorption and mechanical properties of cassava starch films and their relation to plasticizing effect. *Carbohydrate Polymers, 60*(3), 283–289.

Matveev, Y. I., Grinberg, V. Y., & Tolstoguzov, V. B. (2000). The plasticizing effect of water on proteins, polysaccharides and their mixtures. Glassy state of biopolymers, food and seeds. *Food Hydrocolloids, 14*(5), 425–437.

McHugh, T. H., Avena-Bustillo, R., & Krochta, J. M. (1993). Hydrophilic edible films: modified procedure for water vapor permeability and explanation of thickness effects. *Journal of Food Science, 58*(4), 899–903.

Moraes, J. O., Scheibe, A. S., Sereno, A., & Laurindo, J. B. (2013). Scale-up of the production of cassava starch based films using tape-casting. *Journal of Food Engineering, 119*(4), 800–808.

Muriel-Galet, V., López-Carballo, G., Gavara, R., & Hernández-Muñoz, P. (2014). Antimicrobial properties of ethylene vinyl alcohol/epsilon-polylysine films and their application in surimi preservation. *Food and Bioprocess Technology, 7*(12), 3548–3559.

Peltzer, M. A., Salvay, A. G., Delgado, J. F., & Wagner, J. R. (2017). Use of edible films and coatings for functional foods developments: a review. In D. L. Nelson (Ed.), *Functional foods sources, health effects and future perspectives* (pp. 1–26). New York: Nova Science Publishers Inc.

Peltzer, M. A., Delgado, J. F., Salvay, A. G., & Wagner, J. R. (2018a). β-Glucan, a promising polysaccharide for bio-based films developments for food contact materials and medical applications. *Current Organic Chemistry, 22*(12), 1249–1254.

Peltzer, M. A., Salvay, A. G., Delgado, J. F., de la Osa, O., & Wagner, J. R. (2018b). Use of residual yeast cell wall for new biobased materials production: Effect of plasticization on film properties. *Food and Bioprocess Technology, 11*(11), 1995–2007.

Re, R., Pellegrini, N., Proteggente, A., Pannala, A., Yang, M., & Rice-Evans, C. (1999). Antioxidant activity applying an improved ABTS radical cation decolorization assay. *Free Radical Biology and Medicine, 26*(9-10), 1231–1237.

Roy, S., Gennadios, A., Weller, C. L., & Testin, R. F. (2000). Water vapor transport parameters of a cast wheat gluten film. *Industrial Crops and Products, 11*(1), 43–50.

Rozenberga, L., Skute, M., Belkova, L., Sable, I., Vikele, L., Semjonovs, P., Saka, M., Ruklisha, M., & Paegle, L. (2016). Characterisation of films and nanopaper obtained from cellulose synthesised by acetic acid bacteria. *Carbohydrate Polymers, 144*, 33–40.

Salvay, A. G., Colombo, M. F., & Grigera, J. R. (2003). Hydration effects on the structural properties and haem-haem interactions in haemoglobin. *Physical Chemistry Chemical Physics, 5*(1), 192–197.

Sangatash, M. M., Niazmand, R., Jamab, M. S., & Modaressi, A. S. (2016). Development of antioxidant active films containing sodium ascorbate (SA) and ethylene vinyl alcohol (EVOH) to extend the shelf life of peanut. *Journal of Food Science and Technology, 53*, 1766–1783.

Siracusa, V., Rocculi, P., Romani, S., & Rosa, M. D. (2008). Biodegradable polymers for food packaging: a review. *Trends in Food Science and Technology, 19*(12), 634–643.

Smith, W. F. (1997). *Fundamentos de la ciencia e ingeniería de materiales. Segunda edición en español*. Madrid: McGraw Hill.

Song, J., Birbach, N., & Hinestroza, J. (2012). Deposition of silver nanoparticles on cellulosic fibers via stabilization of carboxymethyl groups. *Cellulose, 19*(2), 411–424.

Šturcová, A., Davies, G. R., Eichhorn, S., & J. (2005). Elastic modulus and stress-transfer properties of tunicate cellulose whiskers. *Biomacromolecules, 6*(2), 1055–1061.

Tashiro, K., & Kobayashi, M. (1991). Theoretical evaluation of three-dimensional elastic constants of native and regenerated celluloses: role of hydrogen bonds. *Polymer, 32*(8), 1516–1526.

Wang, L., Dong, Y., Men, H., Tong, J., & Zhou, J. (2013). Preparation and characterization of active films based on chitosan incorporated tea polyphenols. *Food Hydrocolloids, 32*(1), 35–41.

Wu, J., Sun, X., Guo, X., Ji, M., Wang, J., Cheng, C., Chen, L., Wen, C., & Zhang, Q. (2018). Physicochemical, antioxidant, in vitro release, and heat sealing properties of fish gelatin films incorporated with β-cyclodextrin/curcumin complexes for apple juice preservation. *Food and Bioprocess Technology, 11*(2), 447–461.

Xia, Z., Singh, A., Kiratitanavit, W., Mosurkal, R., Kumar, J., & Nagarajan, R. (2015). Unraveling the mechanism of thermal and thermo-oxidative degradation of tannic acid. *Thermochimica Acta, 605*, 77–85.n.